

Original Research

Identification of novel targets of miR-622 in hepatocellular carcinoma reveals common regulation of cooperating genes and outlines the oncogenic role of zinc finger CCHC-type containing 11[☆]

CrossMark

Anne Gaza^{a,b,c}; Valerie Fritz^{a,b}; Lara Malek^a;
Laura Wormser^{a,b}; Nora Treiber^d; Johannes Danner^d;
Andreas E. Kremer^{b,c}; Wolfgang E. Thasler^e;
Jürgen Siebler^{b,c}; Gunter Meister^d;
Markus F. Neurath^{b,c,f}; Claus Hellerbrand^{a,f};
Anja K. Bosserhoff^{a,f}; Peter Dietrich^{a,b,c,*}

^a Institute of Biochemistry, Emil-Fischer-Zentrum, Friedrich-Alexander-University Erlangen-Nürnberg, Erlangen, Germany

^b Department of Medicine, University Hospital Erlangen, Friedrich-Alexander-University Erlangen-Nürnberg, Erlangen, Germany

^c Deutsches Zentrum für Immuntherapie (DZI), Friedrich-Alexander-University Erlangen-Nürnberg and University Hospital Erlangen, Erlangen, Germany

^d Biochemistry Center Regensburg, Laboratory for RNA Biology, University of Regensburg, Germany

^e Department of General and Visceral Surgery, Red Cross Hospital of Munich, Germany

^f Comprehensive Cancer Center (CCC) Erlangen-EMN, Erlangen, Germany

Abstract

The poor prognosis of advanced hepatocellular carcinoma (HCC) is driven by diverse features including dysregulated microRNAs inducing drug resistance and stemness. Lin-28 homolog A (LIN28A) and its partner zinc finger CCHC-type containing 11 (ZCCHC11) cooperate in binding, oligouridylation and subsequent degradation of tumorsuppressive let-7 precursor microRNAs. Functionally, activation of LIN28A was recently shown to promote stemness and chemoresistance in HCC. However, the expression and regulation of LIN28A in HCC had been unclear. Moreover, the expression, regulation and function of ZCCHC11 in liver cancer remained elusive.

In contrast to "one-microRNA-one-target" interactions, we identified common binding sites for miR-622 in both LIN28A and ZCCHC11, suggesting miR-622 to function as a superior pathway regulator. Applying comprehensive microRNA database screening, human hepatocytes and HCC cell lines, patient-derived tissue samples as well as "The Cancer Genome Atlas" (TCGA) patient cohorts, we demonstrated that loss of tumorsuppressive miR-622 mediates derepression and overexpression of LIN28A in HCC. Moreover, the cooperator of LIN28A, ZCCHC11, was newly identified as a prognostic and therapeutic target of miR-622 in liver cancer. Together, identification of novel miR-622 target genes revealed common regulation of cooperating genes and outlines the previously unknown oncogenic role of ZCCHC11 in liver cancer.

Neoplasia (2021) 23, 502–514

Keywords: Hepatocellular carcinoma, HCC, microRNA, drug resistance, ZCCHC11

Introduction

Worldwide increasing incidence rates and emerging but still limited therapeutic options underline that hepatocellular carcinoma (HCC) is a serious global health problem [1,2]. In recent years, novel and most promising systemic therapeutic options were approved for HCC in advanced and

Abbreviations: CNTLT, corresponding nontumorous liver tissues; HCC, hepatocellular carcinoma; LIN28A, Lin-28 homolog A; TMA, tissue micro arrays; ZCCHC11, zinc finger CCHC-type containing 11.

* Corresponding author.

E-mail address: peter.dietrich@fau.de (P. Dietrich).

☆ Declaration of competing interest: All authors declare that no conflict of interest exists.
Received 22 December 2020; received in revised form 1 April 2021; accepted 6 April 2021

intermediate stages [3–5]. As a result, the therapeutic landscape of HCC will change dramatically in the next years [6–9]. However, the prognosis of patients with advanced HCC is still poor, which is mainly driven by diverse mechanisms driving primary and acquired drug resistance [10,11].

It has been demonstrated by our group and others that microRNAs (miRs) represent powerful small RNA molecules that modulate drug resistance related features in HCC [12–14]. Moreover, negative regulators of tumorsuppressive microRNAs can promote cancer progression [15]. Therefore, noncoding RNAs are considered as potent emerging tools with numerous potential clinical applications in HCC [13,16].

We had shown previously that the potent tumorsuppressor miR-622 is lost in HCC, thereby promoting sorafenib resistance by inducing KRAS overexpression [13,17,18]. However, in HCC, by now only three direct miR-622-targets have been identified (i.e., mitogen-activated protein 4 kinase 4 (MAP4K4), CXC chemokine receptor 4 (CXCR4), and kirsten rat sarcoma (KRAS) [17,19,20].

Since the majority of miR-622-targets remained elusive in HCC, we aimed at deciphering novel target genes and pathways of this powerful microRNA.

Results

Common binding sites in cooperating genes suggest miR-622 to function as a superior pathway regulator

According to our aim to identify further drug resistance and/or stemness related target genes of miR-622 in HCC, we performed extensive in silico screening applying several miR-target interaction databases ("miRTarBase 2020"; "miRDB"; "TargetScan"; "miRNAMAP 2.0") [21–24], "string" pathway analysis [25] and comprehensive literature search applying Medline/PubMed and the key terms "cancer", "stemness", "drug resistance", "liver cancer", "hepatocellular carcinoma" and "microRNA". We found that miR-622 potentially regulates numerous oncogenic target genes in HCC (Fig. 1A). Unexpectedly, among these candidate targets, we identified one pair of directly interacting, functionally synergistic pathway genes (lin-28 homolog A (LIN28A) and zinc finger CCHC-type containing 11 (ZCCHC11)) that might be commonly regulated by miR-622 (Fig. 1A).

LIN28A was shown to bind to the strong tumorsuppressive let-7 precursor miRNA (pre-let-7), thereby inducing its degradation [15]. Degradation of pre-let-7 is mediated by the LIN28-cooperating partner ZCCHC11, which promotes oligouridylation and exosomal degradation of pre-let-7 [15,26]. By now, the expression and regulation of LIN28A remained elusive in HCC. Moreover, the potential role of ZCCHC11 in HCC was unknown.

Since miR-622 might "cotarget" both LIN28A and ZCCHC11, we hypothesized that loss of miR-622 in HCC [17,19,20] might de-repress the stemness and resistance-associated LIN28A-ZCCHC11-axis in HCC in the sense of a superior network regulator (Fig. 1B).

LIN28A is overexpressed in human liver cancer

Recently, LIN28A activation was shown to be associated with stemness and chemoresistance in HCC [27]. Apart from this single study on LIN28A function, the expression of LIN28A remained poorly described in HCC. Moreover, a potential regulation by miR-622 was unknown.

Therefore, we first focused on LIN28A expression and the analysis of its cellular localization pattern in HCC. As compared to primary human hepatocytes, LIN28A was strongly upregulated in human HCC cell lines (HepG2, Hep3B, PLC) in vitro (Fig. 2A). LIN28A can be localized both in the nucleus and in the cytoplasm [15], however, its oncogenic function is mediated mainly via cytoplasmatic binding of pre-let-7 [15,26]. To determine the (sub)cellular localization pattern in HCC cells, we applied a

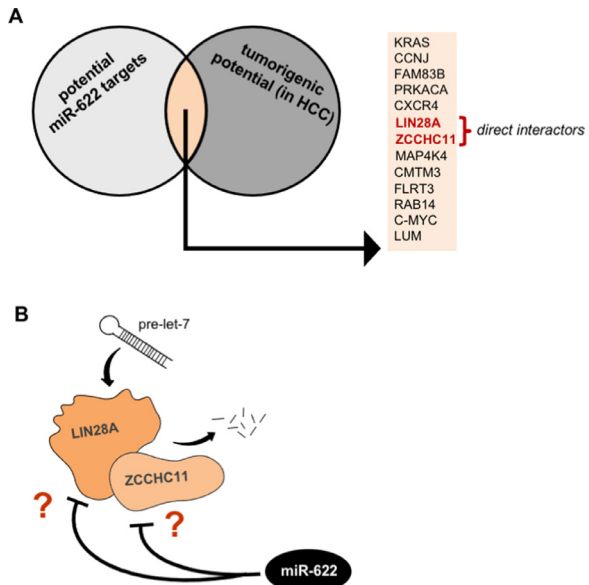


Fig. 1. Common binding sites in cooperating genes suggest miR-622 to function as a superior pathway regulator in HCC. (A) In silico screening strategy for identification of further drug resistance and/or stemness related target genes of miR-622 in HCC. Potential novel miR-622 targets were predicted applying miR-target interaction databases ("miRTarBase 2020"; "miRDB"; "TargetScan"; "miRNAMAP 2.0"), "string" pathway analysis, and comprehensive literature search applying Medline/PubMed (key terms: "cancer", "stemness", "drug resistance", "liver cancer", "hepatocellular carcinoma" and "microRNA"). (B) Hypothesis of potential regulation of both LIN28A and ZCCHC11 by miR-622 in HCC. Binding of let-7 precursors (pre-let-7) by LIN28A and subsequent oligouridylation by its cooperating partner ZCCHC11 was described to induce depletion of let-7-miRNA [15].

LIN28A-isoform-specific antibody as established before [28,29]. Antibody-specificity was confirmed applying a LIN28A-overexpression vector plasmid (Fig. 2B,C). Functionally, forced overexpression of LIN28A confirmed enhanced clonogenicity in HCC cells [27] (Suppl. Fig. 1A). Moreover, qRT-PCR analyses comparing nonresistant and Sorafenib-resistant cell lines (PLC, Hep3B) that are well-established in our laboratory [17] confirmed overexpression of LIN28A in acquired drug resistance in HCC. (Suppl. Fig. 1B).

Subsequent immunofluorescence analysis revealed exclusive cytoplasmatic localization of LIN28A in human HCC cell lines (Fig. 2D). Predominant cytoplasmatic localization of LIN28A was also confirmed in several non-HCC cancer cell lines applying the human ProteinAtlas database [30–32] (Suppl. Fig. 1C,D).

In vivo, LIN28A mRNA levels were found to be significantly upregulated in HCC patient samples as compared to corresponding nontumorous liver tissues (Fig. 2E). Also, on the protein level, analysis of a patient-derived tissue micro arrays (TMA) confirmed enhanced LIN28A expression in HCC as compared with corresponding nontumorous liver tissues as well as a predominant cytoplasmatic staining pattern (Fig. 2F,G,H; Suppl. Tab.1). Furthermore, clinicopathologic correlation analysis revealed that strong LIN28A staining was associated with in advanced tumor stages (Fig. 2I; Suppl. Tab.2).

LIN28A is a novel target gene of miR-622 in HCC

Next, in silico-based analyses confirmed the predicted conserved microRNA response elements (MRE) for miR-622 within the 3'UTR of

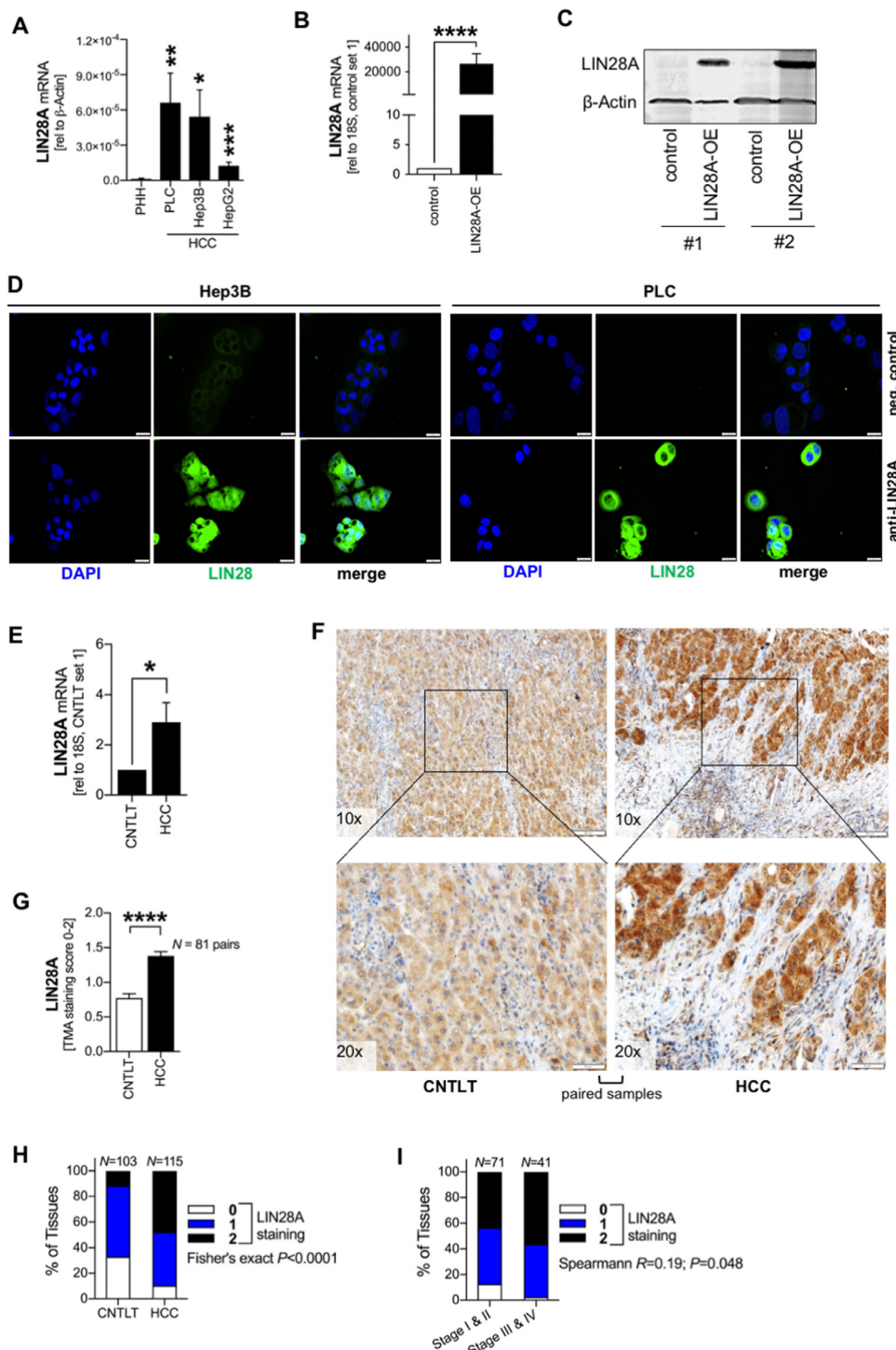


Fig. 2. LIN28A is overexpressed in human liver cancer. (A) Quantitative RT-PCR analysis of LIN28A mRNA levels in primary human hepatocytes (PHH) ($n = 10$) as compared with human HCC cell lines (PLC ($n = 9$), Hep3B ($n = 10$), HepG2 ($n = 11$)). (B,C) Quantitative RT-PCR analysis (A) and representative Western blot images depicting LIN28A mRNA and recombinant protein expression, respectively, after transfection of HepG2 cells (low endogenous LIN28A expression as compared with PLC and Hep3B) applying a LIN28A-overexpression (OE) plasmid vector (provided by G. Meister and described in detail elsewhere [29] ($n = 4$)). (D) Immunofluorescence analysis of LIN28A expression and localization in two different HCC cell lines (PLC ($n = 2$), Hep3B ($n = 2$)) (representative images, 40-fold magnification). (E) LIN28A mRNA levels (qRT-PCR analysis) of paired human HCC and corresponding nontumorous liver tissue (CNTLT) samples ($n = 10$ pairs). (F-I) Immunohistochemical analysis of LIN28A protein expression and cellular localization patterns in patients applying tissue micro array derived paired HCC tissues and CNTLT. Staining intensity and percentage of positive cells were incorporated into a semiquantitative score describing "0" (very low/no expression), "1" (low/moderate expression) and "2" (strong expression). (F) depicts representative immunohistochemical images. (G) LIN28A protein expression score in human HCC tissues and CNTLT applying a tissue micro array (paired analyses). (H) LIN28A expression in HCC ($n = 103$) as compared with CNTLT ($n = 115$) (semiquantitative analysis applying Fisher's exact test). (I) Spearman correlation analysis of LIN28A expression levels in HCC patients with early (stage I & II) ($n = 71$) compared with late (stage III and IV) tumor stages (UICC 2010). Data are presented as the mean \pm SEM. Statistical significance was determined by 2-tailed, unpaired t-test (A,B), paired t-test (E,G), by two-sided Fisher's exact test (H), and Spearman correlation (I). * $P < 0.05$, ** $P < 0.01$, *** $P < 0.001$, **** $P < 0.0001$.

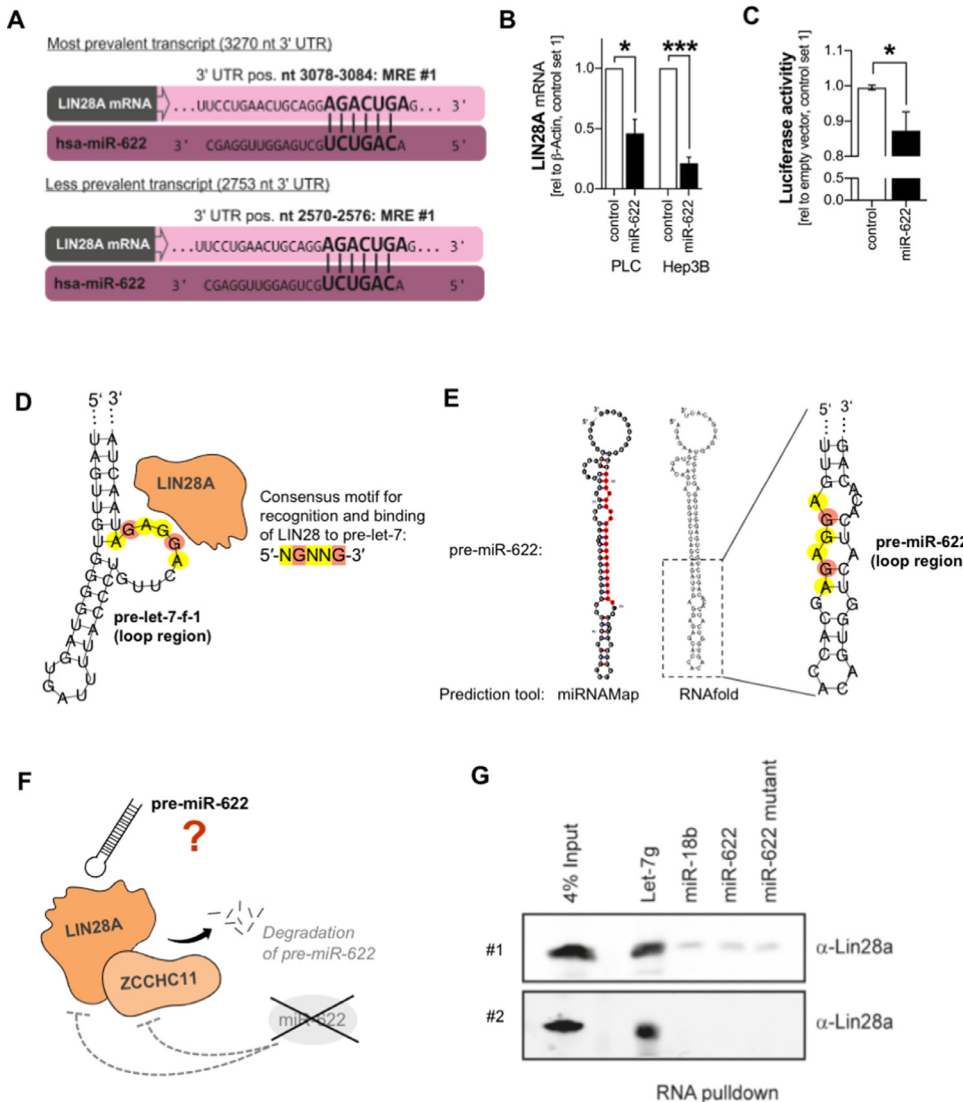


Fig. 3. LIN28A is a novel target gene of miR-622 in HCC. (A) MicroRNA recognition elements (MRE) in the LIN28A 3'UTR represent potential miR-622-binding sites and were identified applying the "TargetScan 7.2" database. (B) Quantitative RT-PCR analysis of LIN28A mRNA levels in control-transfected as compared to miR-622-transfected different HCC cell lines (PLC ($n = 3$); Hep3B ($n = 3$)). (C) Luciferase LIN28A 3'UTR-reporter (containing a conserved miR-622 MRE) activity in control-miR (CTR) as compared with miR-622-mimic (622)-transfected HCC cells (PLC) ($n = 3$). (D) Schematic image depicting the pre-let-7-f-1 loop region (as predicted applying RNA-fold [80] with the highlighted consensus motif for recognition and binding of LIN28 to pre-let-7-f-1 which was identified previously [33]. (E) Schematic image depicting the pre-miR-622 stem loop (as predicted applying RNA-fold [80] and miRNAMap [24]) and magnification of the pre-miR-622 loop region containing the identic sequence motif as identified previously for recognition and binding of LIN28 to pre-let-7. (F) Hypothesis image: According to pre-let-7, LIN28A might also bind to the terminal loop of pre-miR-622 with subsequent ZCCHC11-mediated oligouridylation followed by degradation of pre-miR-622. (G) RNA-pulldown ($n = 2$) depicting binding of LIN28A to the let-7-g hairpin (positive control). No binding was found applying a negative control miR without the potential consensus motif (miR-18b) as well as a miR-622 and a miR-622-mutated (mutated consensus motif) hairpin. Data are presented as the mean \pm SEM. Statistical significance was determined by 2-tailed, unpaired t-test (A,B). * $P < 0.05$, *** $P < 0.001$.

LIN28A mRNA transcripts (but not in its homolog LIN28B) (Fig. 3A). Quantitative RT-PCR analysis applying two different HCC cell lines (PLC, Hep3B) revealed significantly reduced LIN28A mRNA expression levels after re-expression of miR-622 (Fig. 3B). Moreover, the novel miR-622-LIN28A-interaction was mechanistically proven applying a Luciferase reporter gene construct containing the predicted miR-622 MRE (Fig. 3C).

Conversely, the 5'-NGNNG-3' sequence had been demonstrated to be a consensus motif within the loop region of let-7 precursors for selective recognition and binding of LIN28 to pre-let-7 family members

[33] (Fig. 3D). Of note, the identic sequence was identified within the loop region of pre-miR-622 (Fig. 3E). Moreover, the consensus motif was repeatedly detected within the stem region of pre-miR-622 (Suppl. Fig. 1E). We tested the hypothesis that LIN28A might also bind to its negative regulator miR-622, resulting in a double-negative inhibition loop (Fig. 3F). The pre-miR-622 hairpin containing the putative LIN28A-binding site located within the loop region as well as a mutant-hairpin was constructed (Suppl. Fig. 1F). However, subsequent RNA pull down assays did not support the model of a potential double-negative feedback mechanism (Fig. 3G).

Together, the stemness associated homolog of LIN28 (LIN28A) was found to be strongly overexpressed and localized to the cytoplasm of human liver cancer cells in vitro and in vivo. Moreover, LIN28A was shown to be a novel direct target gene of miR-622 in HCC.

ZCCHC11 is overexpressed in HCC

Cytoplasmatic LIN28A interacts with the terminal uridylyltransferase ZCCHC11 to induce degradation of the tumorsuppressor pre-miR-let-7 [15,26]. However, the expression, function and regulation of ZCCHC11 in HCC remained unknown. According to our initial screen, we proposed a "dual" regulation of the resistance and stemness associated LIN28A-ZCCHC11-axis by miR-622 in HCC. In vitro, qRT-PCR analysis revealed marked upregulation of ZCCHC11 mRNA levels in HCC cells as compared with primary human hepatocytes (Fig. 4A). Western blot analysis confirmed overexpression of ZCCHC11 protein levels in human HCC cells (Fig. 4B). Moreover, analysis of HCC patient tissues and corresponding nontumorous liver tissues revealed significant upregulation of ZCCHC11 on the mRNA level (Fig. 4C), which was also confirmed by assessing an additional TCGA cohort (Fig. 4D). Also on the protein level, further analyses applying the human ProteinAtlas database [30–32] revealed specific and marked overexpression as well as a cytoplasmatic localization pattern in HCC as compared with nontumor liver tissues (Fig. 4E) or non-HCC liver tumors (Suppl. Fig. 2A). Predominant cytoplasmatic localization of ZCCHC11 was also found in non-HCC cancer cells (Suppl. Fig. 2B). To confirm these findings in larger patient cohorts, we applied our tissue micro array containing paired HCC and nontumorous liver tissues, and found significant upregulation and cytoplasmatic localization of ZCCHC11 protein levels in human HCC (Fig. 4F,G,H; Suppl. Tab.1; Suppl. Tab.2).

ZCCHC11 displays oncogenic functions in HCC

To determine the functional effects of ZCCHC11 in HCC, specific gene knockdown was performed applying an innovative si-RNA-pooling-technology (siPools, a pool comprising 30 target-specific single si-RNAs allowing highly specific gene silencing while off-target effects of individual si-RNAs are reduced to a minimum [34]) (Fig. 5A). In human HCC cells, ZCCHC11 knockdown induced slight, but nonsignificant reduction of migration and clonogenicity in HCC cells (Fig. 5B,C). In contrast, knockdown of ZCCHC11 markedly reduced proliferation of HCC cells (Fig. 5D). According to the specific effects on proliferation in vitro, ZCCHC11 expression levels in HCC tissues strongly correlated with different cyclins (Cyclin D1, Cyclin D3) and multiple cyclin-dependent kinases (CDK1-10, CDK12-13, CDK16-20) which represent well-known proliferation- and cell cycle promotors in liver cancer [35,36] (Fig. 5E; Suppl. Fig. 3A). Next to cell cycle promotors, correlation analyses applying TCGA datasets revealed a strong association of ZCCHC11 expression levels with markers of hypoxia and neovascularization including HIF1A, ANGPT2 and VEGFA in HCC tissues (Suppl. Fig. 4B). Accordingly, further upregulation of ZCCHC11 was detected under hypoxic conditions in HCC cells (Suppl. Fig. 4C). In contrast, a potential regulation of its partner LIN28A by hypoxia was not detected in HCC cell lines (Suppl. Fig. 4D).

Moreover, TCGA-derived patient cohort analysis (applying the Gene Expression Profiling Interactive Analysis (GEPIA) database [37] and the ProteinAtlas database [30–32] indicated that high ZCCHC11 expression is associated with poor overall survival in HCC (Fig. 5F,G).

In summary, these data revealed that ZCCHC11 is strongly overexpressed in HCC, promotes cancer cell proliferation and is associated with poor survival. We concluded that ZCCHC11 represents a potential novel therapeutic target in HCC.

ZCCHC11 is regulated by miR-622 in HCC

As described, we had identified the ZCCHC11-partner LIN28A as a novel miR-622-target gene in HCC. Tissue micro array analysis revealed strong couregulation of LIN28A and ZCCHC11 in liver cancer (Fig. 6A; Suppl. Tab.2), supporting a common regulatory mechanism. Aiming to identify a (further) mechanism driving the marked overexpression of ZCCHC11 in HCC, we elucidated whether miR-622 is also a direct regulator of ZCCHC11 according to our initial in silico-based prediction and hypothesis. We identified two conserved miR-622-MRE within the 3'UTR of the ZCCHC11 mRNA (Fig. 6B). After miR-622 re-expression, qRT-PCR analysis revealed that ZCCHC11 mRNA levels were downregulated in HCC cell lines (PLC, Hep3B) (Fig. 6C). Moreover, applying Western blot analysis showed marked inhibition of ZCCHC11 protein expression in miR-622-transfected HCC cell lines as compared to control-treated cells (Fig. 6D). Subsequently, the newly defined miR-622-ZCCHC11-interaction was proven mechanistically applying a Luciferase reporter construct by cloning of miR-622 MRE#1 of ZCCHC11 into the vector (Fig. 6E). Furthermore, analysis of TCGA datasets revealed that in HCC patients, high ZCCHC11 and low miR-622 levels (indicated by an elevated ZCCHC11/miR-622-ratio as compared to a low ZCCHC11/miR-622-ratio) were associated with a poor overall survival (Fig. 6F). Conversely, a high miR-622/ZCCHC11-ratio (as compared with a low miR-622/ZCCHC11-ratio) was associated with a better overall survival (Fig. 6G).

In summary, ZCCHC11 was found to be strongly overexpressed in HCC. Our analyses indicate ZCCHC11 as a novel direct target of miR-622 and point to ZCCHC11 as a novel prognostic and therapeutic target in HCC.

Discussion

In recent years, miR-622 has emerged as one of the most promising tumorsuppressive microRNAs, which is underscored by numerous studies addressing its potent role in diverse types of cancer [13,17,18,20,38–44].

In contrast, so far only three studies have identified and experimentally proved target genes of miR-622 in liver cancer (i.e., mitogen-activated protein 4 kinase 4 (MAP4K4), CXC chemokine receptor 4 (CXCR4), and kirsten rat sarcoma (KRAS) [17,19,20]. Regarding the fact that one single microRNA can regulate a target gene network composing of hundreds of mRNAs [13,45], the majority of miR-622-targets in liver cancer remained elusive. Applying comprehensive microRNA database and literature screening, we predicted numerous potential oncogenic candidate target genes of miR-622 in HCC. Unexpectedly, we identified a pair of functionally synergistic, directly interacting genes that might be commonly regulated by miR-622.

Subsequently, the synergistic interactors ZCCHC11 and LIN28A were both identified as novel target genes of miR-622 in liver cancer. To the best of our knowledge, a common regulation of directly cooperating genes by the same microRNA has not been described before in HCC or other types of cancer.

LIN28A and LIN28B are overexpressed in approx. 20% of human cancers, and overexpression of either protein can induce increased cancer aggression and poor prognosis [15]. LIN28B is a well-known cancer promotor and had been characterized recently to be associated with drug response in HCC [46]. Moreover, LIN28B was upregulated in HCC tissues, and high LIN28B expression was associated with high α -fetoprotein levels and shorter overall survival in HCC patients [47]. Furthermore, LIN28B was described to be a tumor marker and to be associated with tumor recurrence in HCC [48–50].

In contrast to LIN28B, only its homolog LIN28A revealed miR-622 binding sites. However, LIN28A was yet poorly described in HCC but was recently shown to be functionally associated with stemness and chemoresistance in liver cancer [27]. In this study, LIN28A was found to

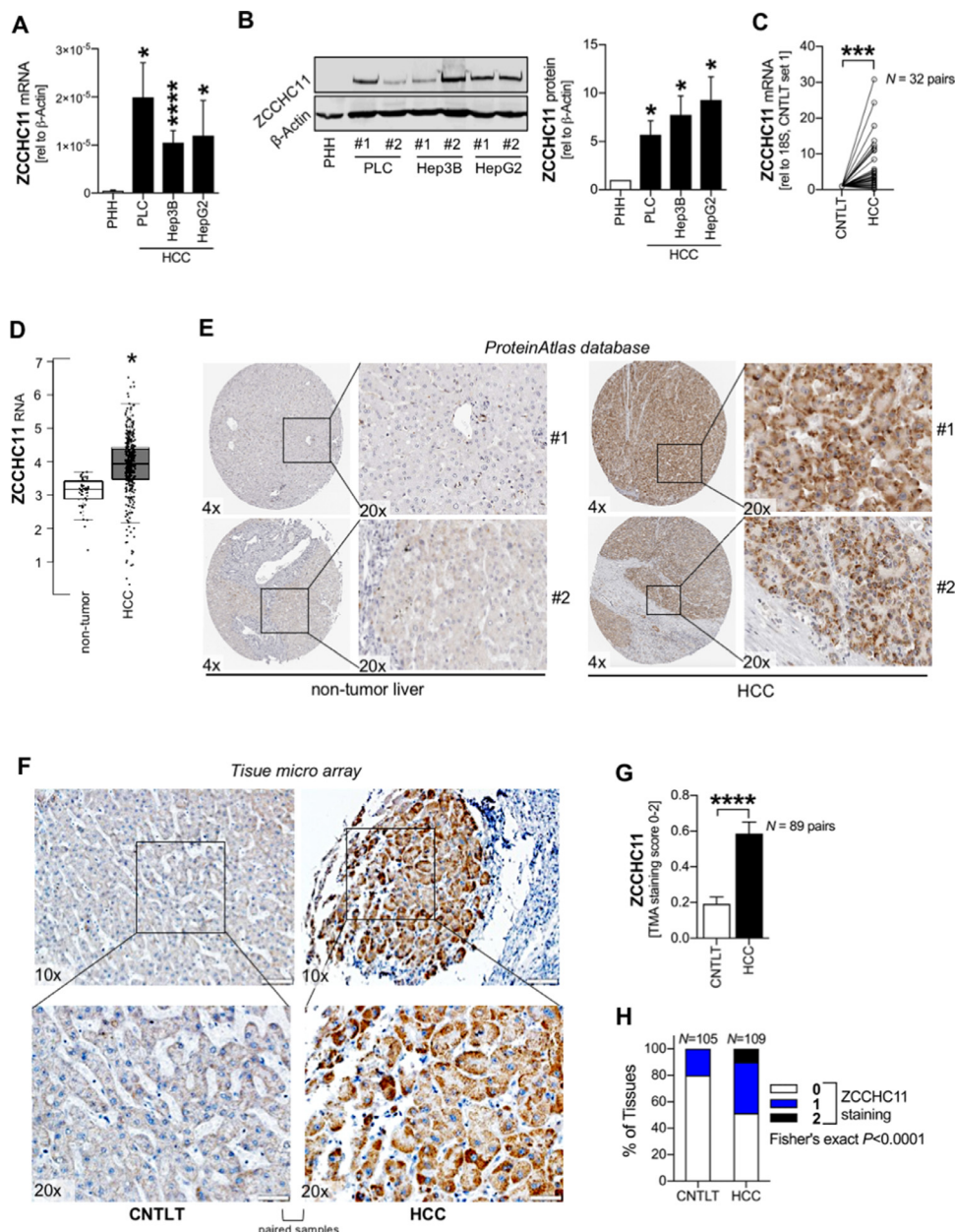


Fig. 4. ZCCHC11 is overexpressed in HCC. (A) Quantitative RT-PCR analysis of ZCCHC11 mRNA levels in primary human hepatocytes (PHH) ($n = 9$) as compared with human HCC cell lines (PLC ($n = 10$), Hep3B ($n = 6$), HepG2 ($n = 15$))). (B) Representative Western blot image and (densitometric) quantification of ZCCHC11 protein levels in PHH ($n = 3$) as compared with human HCC cell lines (PLC ($n = 4$), Hep3B ($n = 4$), HepG2 ($n = 4$))). (C) ZCCHC11 mRNA levels (qRT-PCR analysis) in paired human HCC tissue samples and corresponding nontumorous liver tissues (CNTLT) ($n = 32$ pairs). (D) Transcriptomics data of ZCCHC11 RNA expression levels in HCC ($n = 369$) and nontumorous liver tissues ($n = 50$) derived from TCGA-data applying the Gene Expression Profiling Interactive Analysis (GEPIA) database. (E) ZCCHC11 overexpression in HCC tissues ($n = 2$) as compared with nontumorous liver tissues ($n = 2$) applying the human proteinatlas database (representative images). (E-H) Confirmation of ZCCHC11 protein expression and cellular localization patterns in patients applying tissue micro array derived paired HCC tissues and CNTLT. Staining intensity and percentage of positive cells were incorporated into a semi-quantitative score describing "0" (very low/no expression), "1" (low/moderate expression) and "2" (strong expression). (H) Representative immunohistochemistry images and paired quantification of ZCCHC11 expression score (G) as well as semiquantitative analysis applying Fisher's exact test (H) in HCC as compared with CNTLT. Data are presented as the mean \pm SEM. Statistical significance was determined by 2-tailed, unpaired t-test (A,B,D), paired t-test (G), and two-sided Fisher's exact test (H). * $P < 0.05$, *** $P < 0.001$, **** $P < 0.0001$.

be a novel target gene of miR-622 in HCC and was strongly overexpressed and localized to the cytoplasm (which was previously determined to be crucial for its interaction with ZCCHC11 and its oncogenic function) of human liver cancer cells. Our findings underscore that next to the well-

known promotor of HCC, LIN28B, also its poorly described homolog LIN28A contributes to liver cancer progression and drug resistance via specific regulatory mechanisms, since miR-622 specifically regulates LIN28A and not LIN28B.

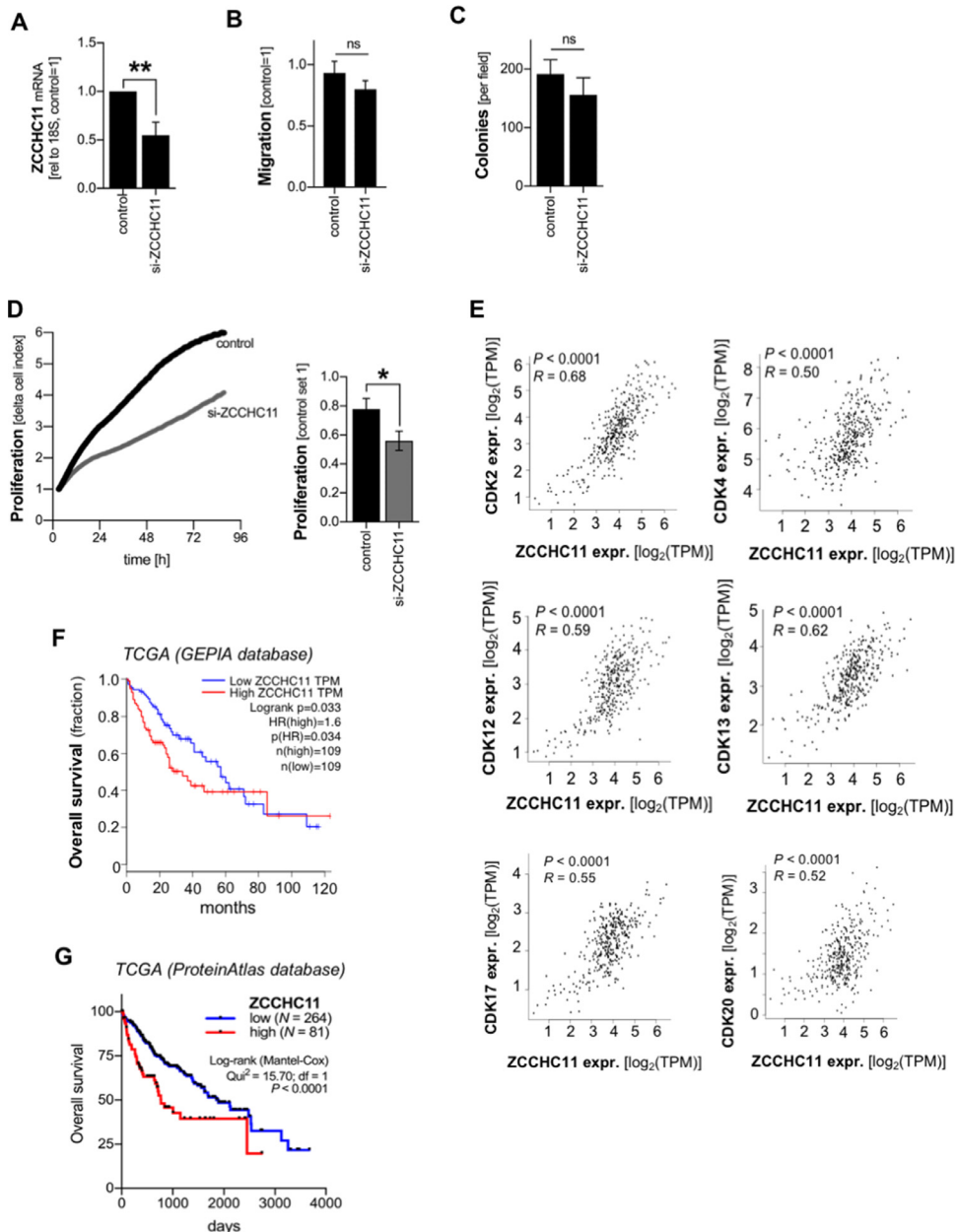


Fig. 5. ZCCHC11 reveals oncogenic functions in HCC. (A-C) HCC cell lines (Hep3B ($n = 2$), PLC ($n = 2$)) were transfected with a control si-RNA-pool or with a specific si-RNA-pool targeting ZCCHC11 for 48 h. (A) ZCCHC11 mRNA levels as determined by qRT-PCR analysis. (B) Migration as determined applying Boyden chamber cell migration assays. (C) Colony numbers as determined applying clonogenic assays. (D) Real-time cell proliferation analysis of HCC cells transfected with an si-RNA-Pool directed against ZCCHC11 or a control si-RNA-Pool ($n = 4$). (E) Correlated ZCCHC11 and CDK2, CDK4, CDK12, CDK14, CDK17, CDK20 RNA expression levels ($\log_2(\text{TPM})$), respectively, in HCC tissues. TCGA-derived data were used applying the Gene Expression Profiling Interactive Analysis (GEPIA) database. The data represent RNA expression levels ($\log_2(\text{TPM})$) in HCC tissues. (F,G) TCGA-derived datasets deposited on the Gene Expression Profiling Interactive Analysis (GEPIA) database (F) or the ProteinAtlas database (G), respectively. "HR": Hazard ratio. Data are presented as the mean \pm SEM. Statistical significance was determined by 2-tailed, unpaired t-test (A,B,C,D) and Pearson correlation analysis (E). Survival analysis was performed computationally applying log-rank testing and hazard ratio estimates (F) or applying log-rank testing (Mantel-Cox) (G). * $P < 0.05$, ** $P < 0.01$, ns: non-significant.

Interestingly, the 5'-NGNNG-3' sequence, which was identified as the consensus motif for selective recognition and binding of LIN28 to pre-let-7 family members [15,33], was also found in the pre-miR-622 sequence. However, a potential mutual double-negative feedback regulation of LIN28A and miR-622 was excluded in our study.

Until now, the function of ZCCHC11 was only poorly described in most types of cancer, and its potential role in liver cancer remained elusive. Our study identified ZCCHC11 as a novel target gene of miR-622 in HCC. Moreover, ZCCHC11 was found to be strongly overexpressed in liver cancer in vitro and in vivo and was shown to drive HCC progression and proliferation.

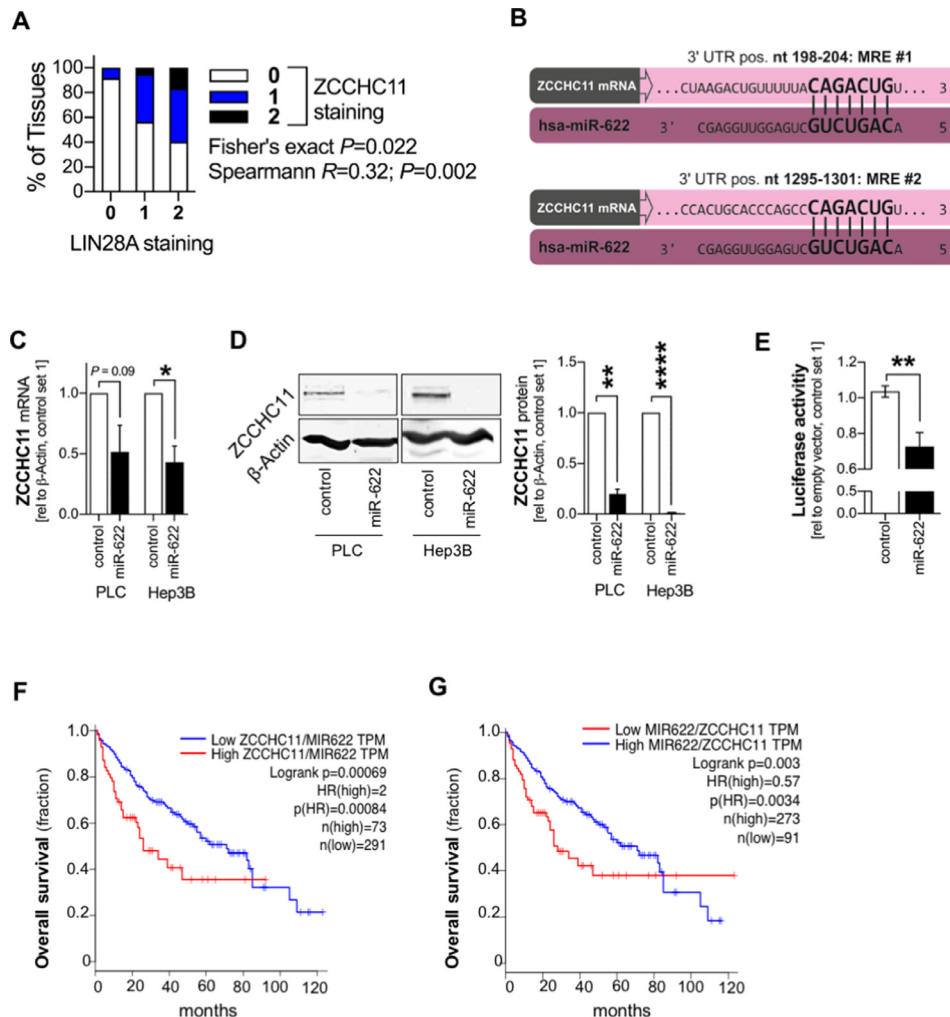


Fig. 6. ZCCHC11 is regulated by miR-622 in HCC. (A) Immunohistochemical analysis and correlation of ZCCHC11 and LIN28A expression levels applying tissue micro arrays (staining intensity and percentage of positive cells for both ZCCHC11 and LIN28A were incorporated into a semi-quantitative score describing "0" (very low/no expression), "1" (low/moderate expression) and "2" (strong expression)) ($n = 102$). (B) MicroRNA recognition elements (MRE) in the ZCCHC11 3'UTR represent potential miR-622-binding sites and were identified applying the "TargetScan 7.2" database. (C) Quantitative RT-PCR analysis of ZCCHC11 mRNA levels in control-transfected as compared to miR-622-transfected different HCC cell lines (PLC ($n = 2$); Hep3B ($n = 3$)). (D) Representative Western blot images and (densitometric) quantification of ZCCHC11 protein levels in control-transfected as compared to miR-622-transfected different HCC cell lines (PLC ($n = 2$); Hep3B ($n = 2$)). (E) Luciferase ZCCHC11 3'UTR-reporter (containing a conserved miR-622 MRE) activity in control-miR (CTR) as compared with miR-622-mimic (622)-transfected HCC cells (PLC) ($n = 3$). (F,G) TCGA-derived datasets and the Gene Expression Profiling Interactive Analysis (GEPIA) database were used for overall survival analysis comparing high and low ZCCHC11/miR-622-ratios (F) or high and low miR-622/ZCCHC11-ratios (G), respectively in HCC patients. "HR": Hazard ratio. Data are presented as the mean \pm SEM. Statistical significance was determined by two-sided Fisher's exact test together with Spearman correlation analysis (A), and 2-tailed, unpaired t-test (C,D,E). Survival analysis was performed computationally applying log-rank testing and hazard ratio estimates (F,G). * $P < 0.05$, ** $P < 0.01$, *** $P < 0.0001$.

Hypoxia and neovascularization are major pathological mechanisms in HCC driving progression and therapy resistance [51–54], and current first-line therapeutic concepts in HCC (sorafenib, lenvatinib, bevacizumab) majorly target the hypoxia-associated VEGF-tumor-vascularization-axis [53,55]. Moreover, miR-622 was directly linked with hypoxia, VEGF-signaling and (neo-)vascularization in several cancer types including colorectal cancer [42,56,57]. In this regard, we found that the novel and yet undescribed target gene of miR-622 in liver cancer, ZCCHC11, was strongly correlated with hypoxia inducible factor 1, angiopoietin 2 and VEGFA in human HCC tissues. Furthermore, experimental hypoxia significantly upregulated ZCCHC11 in human HCC cells. Therefore, next to miR-622,

hypoxia might further contribute to ZCCHC11 overexpression and function in HCC.

In contrast to liver cancer, several further miR-622 target genes have been described in non-HCC cancer types that might potentially also contribute to HCC progression. For example, loss of miR-622 in gastric cancer promoted cellular invasion and tumor metastasis by targeting inhibitor of growth family, member 1 (ING1) [58]. Interestingly, ING1 isoforms reveal differential expression in HCC [59], but their precise function in HCC remained elusive. Moreover, miR-622 was demonstrated to suppress proliferation, invasion and migration by directly targeting activating transcription factor 2 (ATF2) in glioma cells [60]. Since ATF2 was shown to induce chemoresistance in HCC [61], a potential regulation of ATF2 by miR-622 in HCC might

represent a crucial further mechanism driving liver cancer progression and drug resistance.

Our study demonstrates that combined de-repression of both LIN28A and ZCCHC11 as mediated by loss of miR-622 could mechanistically contribute to stronger activation of the oncogenic LIN28A-ZCCHC11-axis in HCC. Couregulation of synergistic genes represents a well-known hallmark of cancer inducing a competitive edge for malignant cells in specific circumstances including drug resistance. Accordingly, co-overexpression of cooperating partner genes had been described in diverse types of cancer before. For example, co-overexpression of HER2 and HER3 was described to be a predictor of poor survival in breast cancer [62]. Furthermore, co-overexpression of fibroblast growth factor receptors 1, 2 and 4 revealed prognostic significance in gastric cancer [63]. Moreover, co-upregulation of Janus kinase 2 and signal transducer and activator of transcription 5a was revealed to impact mammary cancer cells via epithelial–mesenchymal transition (EMT) [64]. Likewise, co-overexpression of TAZ and YAP was demonstrated to represent an independent predictor of poor prognosis in patients with colorectal cancer [65]. Also in renal cell carcinoma, concomitant overexpression of the EGFR and erbB-2 correlated with dedifferentiation and metastasis [66]. Together, numerous studies support that cancer cells take advantage from simultaneous co-overexpression of cooperating genes.

In summary, we demonstrated de-repression of the synergistic partner genes LIN28A and ZCCHC11 by a common microRNA in HCC and identified ZCCHC11 to represent a novel target gene in HCC. Since recently, small molecule inhibitors of ZCCHC11 uridylyl transferase activity were identified [67], the therapeutic potential of this novel miR-622-target should be addressed in further (preclinical) studies.

Material and methods

Human cells and cell culture

The human hepatocellular carcinoma (HCC) cell lines PLC (ATCC CRL-8024), Hep3B (ATCC HB-8064) and HepG2 (ATCC HB-8065) were described in other studies [17,68]. Primary human hepatocytes (PHH) were isolated and cultured according to the technique described by Lee et al. [69].

Sorafenib-resistant HCC cells (PLC, Hep3B) were generated by incubation with stepwise increasing doses of sorafenib as described elsewhere [17,70]. Sorafenib ("Nexavar") was purchased from Cayman Chemical (Michigan, USA).

Human liver tissue

Paired human HCC tissues and corresponding nontumorous liver tissues (CNTLT) were generated from patients undergoing partial hepatectomy. The tissue samples were instantly snap-frozen and stored at -80°C. Moreover, paraffin-embedded tissues were used to construct TMA for immunohistochemistry analysis as described previously [17,68,71] (Suppl. Tab.1). Human samples were collected with the informed patients' consent obtained by the Biobank at the Hospital of the Ludwig-Maximilians-University Munich, which is subject to the guidelines of the nonprofit state-controlled Human Tissue and Cell Research (HTCR) foundation [71].

RNA isolation and expression analysis

RNA isolation and reverse transcription were performed as described previously [72]. Quantitative reverse-transcription polymerase chain reaction (qRT-PCR) was performed applying specific primers on a Lightcycler 480 system (Roche, Mannheim, Germany). The following primers were used: β-Actin (5'-CTA CGT CGC CCT GGA CTT CGA GC-3' and 5'-GAT GGA GCC GCC GAT CCA CAC GG-3'), 18S (5'-TCT GTG ATG CCC TTA GAT GT CC-3' and 5'-CCA TCC AAT CGG TAG TAG CG-3'), LIN28A

(5'-CGG TGC GGG CAT CTG TAA GT GG-3' and 5'-TGG CCG CCT CTC ACT CCC AAT AC-3'), ZCCHC11 (5'-AGC CAA TCC TGC TGT CTC AA-3' and 5'-GTC TGA AGC AAC CAA AGT AT GA-3').

Transfection of si-RNA-pools and miR-622

Approx. $2-3 \times 10^5$ cells were seeded per well of a six-well culture plate. For RNAi-mediated ZCCHC11 knockdown, we used si-Pool-technique (functionally verified si-RNA-Pool targeting human ZCCHC11; siTOOLS Biotech GmbH, Planegg/Martinsried, Germany) was used. The used si-Pool comprised about 30 target-specific single si-RNAs, allowing for highly efficient gene silencing compared with nontargeting control si-Pool, while off-target effects of individual si-RNAs can be reduced to a minimum [34]. MicroRNA (miRNA) mimics (Ambion by ThermoFisher Scientific, Waltham, MA, USA) were described before [43,70]. Extraction of total RNA and protein followed 48 to 72 h after transfection.

Cloning, luciferase reporter gene assays, and RNA pulldown assay

The wild-type sequence of the LIN28A and ZCCHC11 3' untranslated regions (UTR) spanning the required miR-622 response elements (MREs) were amplified applying PCR and HCC cell-derived cDNA using the Phusion High-Fidelity DNA Polymerase kit (ThermoFisher Scientific, Waltham, MA, USA) and the following primers: LIN28A: 5'-CAG TCT AGA ATT TAT GGG GCG GGA GGG TA-3' and 5'-CAG TCT AGA CCA GTG ATG GGG TCA CCA AA-3'; ZCCHC11: 5'-CAG TCT AGA AGT CCA TTT TCT TTC AGC TG GT-3' and 5'-CAG TCT AGA GCA ACC AAA GTA TGA ATA CA GC-3'). The generated amplicons were inserted into the Luciferase 3' UTR of a pGL3-Promoter Firefly Luciferase reporter vector (Promega Corporation, Madison, WI, USA) via an XbaI restriction site. All plasmid sequences were verified by sequencing. The obtained Firefly Luciferase reporter constructs (FLuc) were cotransfected with pre-miR-622 or nontargeting pre-miR-CTR (Ambion by ThermoFisher Scientific, Waltham, MA, USA) and the wild-type Renilla reporter pRL-TK (RLuc; Promega Corporation, Madison, WI, USA) for normalization by using Lipofectamine 2000 Transfection Reagent (ThermoFisher Scientific, Waltham, MA, USA). FLuc signals were normalized to the corresponding RLuc signals by calculating the RLuc/FLuc ratio and correcting for differences in transfection efficiencies. Luciferase assays were performed as described before [17].

RNA-pulldown assays were established and performed by a collaborating group (AG Meister, Laboratory for Biochemistry, University of Regensburg, Germany) as described in detail elsewhere [29,73].

Western blotting

Cell lysis, protein isolation and Western blots were carried out as specified elsewhere [70,74,75]. The following primary antibodies were used: Anti-β-actin (1:5,000 dilution) (Sigma-Aldrich, St. Louis, USA), anti-ZCCHC11 (1:1,000 dilution) (Proteintech, Rosemont, USA), anti-LIN28A (1:1,000 dilution) (AG Meister, Laboratory for Biochemistry, University of Regensburg, Germany [28,29]). β-Actin served as a reference for normalization. Immunoreactions were visualized applying the BCIP/NBT kit (Invitrogen by Thermo Fisher Scientific, Waltham, MA, USA). Densitometric analysis of scanned Western blot images was performed using "ImageJ" (National Institutes of Health, Bethesda, MD, USA).

Immunohistochemistry and immunofluorescence analysis

Immunohistochemistry analysis was performed applying TMA comprising human patient derived liver cancer tissue samples as described before [70,74,75]. Immunohistochemistry staining was analyzed

semiquantitatively and the according scores were established for each antibody as described [17].

Immunofluorescence assays were performed as described [76]. After seeding the cells in chamber slides (20 000 cells per chamber) and 24 h incubation, cells were fixed with methanol-acetic acid and afterward permeabilized using 0.1% Triton-X-100. Subsequently, the cells were blocked for 1 h using 1% bovine serum albumin/PBS, then incubated over night with specific antibodies. The following primary antibodies were used for immunohistochemistry / immunofluorescence: anti-LIN28A (1:100 dilution) (AG Meister, Laboratory for Biochemistry, University of Regensburg, Germany [28,29]; anti-ZCCHC11 (1:50 dilution) (Proteintech, Rosemont, USA). For staining of the nucleus, DAPI (1:1,000 in 1mg/mL stock solution in 3 % BSA/PBS, Sigma-Aldrich Chemie GmbH, Steinheim, Germany) was used.

Proliferation, migration and clonogenicity assays

Quantification of real-time cell proliferation was performed applying the xCELLigence system (Roche, Mannheim, Germany) as described previously [77]. Cell migration was analyzed applying the Boyden chamber system as described before [78]. Stem cell-like properties were determined performing clonogenicity assays as described elsewhere [79]. Number and size of colonies were determined using the Cell Sense software (Olympus, Tokyo, Japan).

In silico analysis

To explore potential microRNA-622 targets and pathways, the following databases were used: miRTarBase 2020, miRDB, TargetScan, miRNAMap 2.0 and string [21–25]. For analysis of The Cancer Genome Atlas (TCGA) derived datasets, the Gene Expression Profiling Interactive Analysis (GEPIA) database [37] as well as datasets provided by the human ProteinAtlas database [30–32] were used. The expression data are first $\log_2(\text{TPM}+1)$ transformed for differential analysis. Statistical significance was determined by computational log-rank testing and Hazard ratios. The method for differential gene expression analysis was one-way ANOVA. For prediction of 2nd structures of pre-let-7-f-1 and pre-miR-622, miRNAMap 2.0 [24] and RNAfold [80] were used.

Statistical analysis

Results are expressed as mean \pm SEM. The unpaired Student's *t* test or, if appropriate, the one-way analysis of variance (ANOVA) with Dunnett's multiple comparison test was used for comparisons between groups (if not depicted otherwise). For analysis of immunohistochemistry scores, the Fisher's exact test was used. The threshold significance level was $P < 0.05$, with the different levels of significance abbreviated as *: $P < 0.05$, **: $P < 0.01$, ***: $P < 0.001$, ****: $P < 0.0001$ and "ns" for nonsignificant. Spearman and Pearson correlation coefficients, respectively, were used for correlation analyses. Comparison of survival curves obtained from publicly available databases was conducted in silico using Log Rank-tests and Hazard ratio estimates. Calculations were performed using the GraphPad Prism Software (GraphPad Software, San Diego, California, USA).

Author contributions

P.D., A.K.B., C.H., A.G., and V.F. conceived the project, analyzed the data, and wrote the paper. A.G., V.F., L.M., L.W., J.D. and N.T. designed and performed the experiments. A.E.K., G.M., J.S., M.F.N., A.K.B. and C.H. provided material and contributed to data analysis and manuscript creation, respectively. The present work was performed in fulfillment of the requirements for obtaining the degree "Dr. med." (M.D.) for A.G.

Supplementary Fig. 1. LIN28A function and expression in HCC and potential binding motifs for miR-622. (A) Clonogenicity assay (representative image) of HCC cells (PLC) after transfection applying a control-vector plasmid (control) as compared with a LIN28A-overexpression (OE) plasmid vector for 48 h ($n=4$, including three technical replicates (repl.) per independent experiment). (B) Summarized LIN28A mRNA levels as quantified by qRT-PCR analysis in non-resistant PLC ($n=4$) and Hep3B ($n=4$) cells as compared with Sorafenib-resistant (Sora-resistant) PLC ($n=4$) and Hep3B ($n=4$). (C,D) Immunofluorescence images confirming predominant cytoplasmatic localization of LIN28A also in non-HCC stem cell and cancer cell lines (e.g. the neural stem cell line "AF22" (A) and the colorectal adenocarcinoma cell line "CACO-2" (B)) (40-fold magnification). (E) Schematic image depicting the pre-miR-622 stem loop (as predicted applying RNA-fold [80]) and magnification of the pre-miR-622 stem region revealing additional putative consensus motifs as identified previously for recognition and binding of LIN28 to pre-let-7. (F) Summarized depiction of the consensus motif as identified for binding of LIN28 to pre-let-7 [80] (top line), the detailed sequence which had been identified as LIN28-binding site to pre-let-7-f loop region [80] (second line), the putative identic sequence motif which is localized to also to the loop region of pre-miR-622 and which was cloned into a vector for construction of the pre-miR-622 hairpin and subsequent LIN28A-pulldown assays (third line) (see also Fig. 3E), and the G20C, G21C double-mutant which was used as a negative control (see also Fig. 3F).

Supplementary Fig. 2. ZCCHC11 expression in non-HCC liver cancer and cellular localization in non-HCC cancer cells. (A) ZCCHC11 expression (immunohistochemistry) in non-HCC-liver cancer (cholangiocarcinoma, CCC) (representative images ($n=2$) provided by the human proteinatlas database) reveals specific overexpression of ZCCHC11 only in HCC. (B) Immunofluorescence image confirming cytoplasmatic localization of ZCCHC11 (the oncogenic function of ZCCHC11 is mediated mainly via cytoplasmatic binding of pre-let-7) also in non-HCC cancer cells (e.g. the glioblastoma cell line "U251-MG") (40-fold magnification).

Supplementary Fig. 3. Correlation of ZCCHC11 with cell cycle associated cyclins, cyclin-dependent kinases and markers of hypoxia in HCC. (A) TCGA-derived data were used applying the Gene Expression Profiling Interactive Analysis (GEPIA) database. ZCCHC11 expression levels were correlated with cell cycle associated cyclins and cyclin-dependent kinases (CCND1, CCND3, CDK1, CDK3, CDK5-10, CDK14, CDK16, CDK18, CDK19). The data represent RNA expression levels ($\log_2(\text{TPM})$) in HCC tissues. Statistical significance was determined by Pearson correlation analysis. (B) TCGA-derived data were used applying the Gene Expression Profiling Interactive Analysis (GEPIA) database. ZCCHC11 expression levels were correlated with markers of hypoxia (HIF1A, ANGPT2, VEGFA). The data represent RNA expression levels ($\log_2(\text{TPM})$) in HCC tissues. (C) ZCCHC11 mRNA expression (qRT-PCR analysis) in HCC cells (PLC) that were exposed to a hypoxic atmosphere (0.1% O₂). HCC cells (PLC) incubated under normoxic conditions (19% O₂) were used as controls ($n=4$). (D) LIN28A mRNA expression (qRT-PCR analysis) in HCC cells (PLC ($n=3$), Hep3B ($n=3$)) that were exposed to a hypoxic atmosphere (0.1% O₂) as compared with normoxic conditions (19% O₂). Data are presented as the mean \pm SEM. Statistical significance was determined by Pearson correlation analysis (A,B) and by 2-tailed, unpaired t-test (C,D). * $P < 0.05$, ns: non-significant.

Funding

This work was supported by grants from the German Research Association (DFG) (Research Training Group "RTG 1962/1" and FOR 2127 and TRR/SFB 305 (B11, B12) to PD, AB and CH), the German Cancer Aid (Deutsche Krebshilfe to PD and AB), the Wilhelm Sander-Stiftung (No. 2020.048.01, to PD), the Else-Kröner-Fresenius Stiftung (EKFS, to PD), and

the Interdisciplinary Center for Clinical Research (IZKF) Erlangen (to PD and AB). We thank Annette Serwotka, Darleen Schönwälter, Sabrina Freitag and Rudolph Jung for excellent technical assistance.

Acknowledgments

We acknowledge the Human Tissue and Cell Research foundation (HTCR, Regensburg, Germany) for making human tissue available for research, as well as Hepacult GmbH (Planegg / Martinsried, Germany) for providing primary human hepatocytes for *in vitro* studies. We appreciate the provision of suitable samples by the Biobank under administration of HCTR at the Hospital of the Ludwig-Maximilians-University Munich based on extensive data and sample analysis.

Supplementary materials

Supplementary material associated with this article can be found, in the online version, at doi:10.1016/j.neo.2021.04.001.

References

- [1] Llovet JM, Zucman-Rossi J, Pikarsky E, Sangro B, Schwartz M, Sherman M, Gores G. Hepatocellular carcinoma. *Nat Rev Dis Primers* 2016;2:16018.
- [2] Liu Z, Lin Y, Zhang J, Zhang Y, Li Y, Liu Z, Li Q, Luo M, Liang R, Ye J. Molecular targeted and immune checkpoint therapy for advanced hepatocellular carcinoma. *J Exp Clin Cancer Res* 2019;38:447.
- [3] Lee YH, Tai D, Yip C, Choo SP, Chew V. Combinational immunotherapy for hepatocellular carcinoma: radiotherapy, immune checkpoint blockade and beyond. *Front Immunol* 2020;11:56759.
- [4] Pinter M, Jain RK, Duda DG. The current landscape of immune checkpoint blockade in hepatocellular carcinoma: a review. *JAMA Oncol* 2021;7(1):113–23. doi:10.1001/jamaoncol.2020.3381.
- [5] Wang Y, Jiang M, Zhu J, Qu J, Qin K, Zhao D, Wang L, Dong L, Zhang X. The safety and efficacy of lenvatinib combined with immune checkpoint inhibitors therapy for advanced hepatocellular carcinoma. *Biomed Pharmacother* 2020;132:110797.
- [6] Kumar V, Rahman M, Gahtori P, Al-Abbas F, Anwar F, Kim HS. Current status and future directions of hepatocellular carcinoma-targeted nanoparticles and nanomedicine. *Expert Opin Drug Deliv* 2020;1–22. doi:10.1080/17425247.2021.1860939.
- [7] Kim E, Viatour P. Hepatocellular carcinoma: old friends and new tricks. *Exp Mol Med* 2020;52(12):1898–907. doi:10.1038/s12276-020-00527-1.
- [8] Kabashima A, Shimada S, Shimokawa M, Akiyama Y, Tanabe M, Tanaka S. Molecular and immunological paradigms of hepatocellular carcinoma: special reference to therapeutic approaches. *J Hepatobiliary Pancreat Sci* 2021;28(1):62–75. doi:10.1002/jhb.p.874.
- [9] Gordon JD, Kennedy EB, Abou-Alfa GK, Beg MS, Brower ST, Gade TP, Goff L, Gupta S, Guy J, Harris WP, et al. Systemic therapy for advanced hepatocellular carcinoma: ASCO guideline. *J Clin Oncol* 2020;38:4317–45.
- [10] Vogel A, Saborowski A. Current strategies for the treatment of intermediate and advanced hepatocellular carcinoma. *Cancer Treat Rev* 2020;82:101946.
- [11] Marin JJJG, Briz O, Herraez E, Lozano E, Asensio M, Di Giacomo S, Romero MR, Osorio-Padilla LM, Santos-Llamas AI, Serrano MA, et al. Molecular bases of the poor response of liver cancer to chemotherapy. *Clin Res Hepatol Gastroenterol* 2018;42:182–92.
- [12] Liang Y, Liang Q, Qiao L, Xiao F. MicroRNAs modulate drug resistance-related mechanisms in hepatocellular carcinoma. *Front Oncol* 2020;10:920.
- [13] Linck-Paulus L, Hellerbrand C, Bosserhoff AK, Dietrich P. Dissimilar appearances are deceptive-common microRNAs and therapeutic strategies in liver cancer and Melanoma. *Cells* 2020;9(1):114. doi:10.3390/cells9010114.
- [14] Pratama MY, Pascut D, Massi MN, Tiribelli C. The role of microRNA in the resistance to treatment of hepatocellular carcinoma. *Ann Transl Med* 2019;7:577.
- [15] Wang L, Nam Y, Lee AK, Yu C, Roth K, Chen C, Ransey EM, Sliz P. LIN28 zinc knuckle domain is required and sufficient to induce let-7 oligouridylation. *Cell Rep* 2017;18:2664–75.
- [16] Cao P, Jin Q, Feng L, Li H, Qin G, Zhou G. Emerging roles and potential clinical applications of noncoding RNAs in hepatocellular carcinoma. *Semin Cancer Biol* 2020. S1044-579X(20)30191-7. Online ahead of print. doi:10.1016/j.semcaner.2020.09.003.
- [17] Dietrich P, Koch A, Fritz V, Hartmann A, Bosserhoff AK, Hellerbrand C. Wild type Kirsten rat sarcoma is a novel microRNA-622-regulated therapeutic target for hepatocellular carcinoma and contributes to sorafenib resistance. *Gut* 2018;67:1328–41.
- [18] Bantel H, Canbay A. Loss of KRAS control as consequence of downregulated microRNA-622 in hepatocellular carcinoma and its potential therapeutic implication. *Gut* 2018;67:1206–7.
- [19] Song WH, Feng XJ, Gong SJ, Chen JM, Wang SM, Xing DJ, Zhu MH, Zhang SH, Xu AM. microRNA-622 acts as a tumor suppressor in hepatocellular carcinoma. *Cancer Biol Ther* 2015;16:1754–63.
- [20] Liu H, Liu Y, Liu W, Zhang W, Xu J. EZH2-mediated loss of miR-622 determines CXCR4 activation in hepatocellular carcinoma. *Nat Commun* 2015;6:8494.
- [21] Huang HY, Lin YC, Li J, Huang KY, Shrestha S, Hong HC, Tang Y, Chen YG, Jin CN, Yu Y, et al. miRTarBase 2020: updates to the experimentally validated microRNA-target interaction database. *Nucleic Acids Res* 2020;48:D148–54.
- [22] Chen Y, Wang X. miRDB: an online database for prediction of functional microRNA targets. *Nucleic Acids Res* 2020;48:D127–31.
- [23] Agarwal V, Bell GW, Nam JW, Bartel DP. Predicting effective microRNA target sites in mammalian mRNAs. *eLife* 2015;4:e05005. doi:10.7554/eLife.05005.
- [24] Hsu SD, Chu CH, Tsou AP, Chen SJ, Chen HC, Hsu PW, Wong YH, Chen YH, Chen GH, Huang HD. miRNAMap 2.0: genomic maps of microRNAs in metazoan genomes. *Nucleic Acids Res* 2008;36:D165–9.
- [25] Szklarczyk D, Gable AL, Lyon D, Junge A, Wyder S, Huerta-Cepas J, Simonovic M, Doncheva NT, Morris JH, Bork P, et al. STRING v11: protein-protein association networks with increased coverage, supporting functional discovery in genome-wide experimental datasets. *Nucleic Acids Res* 2019;47:D607–13.
- [26] Nam Y, Chen C, Gregory RI, Chou JJ, Sliz P. Molecular basis for interaction of let-7 microRNAs with Lin28. *Cell* 2011;147:1080–91.
- [27] Fang T, Lv H, Wu F, Wang C, Li T, Lv G, Tang L, Guo L, Tang S, Cao D, et al. Musashi 2 contributes to the stemness and chemoresistance of liver cancer stem cells via LIN28A activation. *Cancer Lett* 2017;384:50–9.
- [28] Treiber T, Treiber N, Plessmann U, Harlander S, Daiss JL, Eichner N, Lehmann G, Schall K, Urlaub H, Meister G. A compendium of RNA-binding proteins that regulate microRNA biogenesis. *Mol Cell* 2017;66:270–84 e213.
- [29] Ustianenko D, Chiu HS, Treiber T, Weyn-Vanherenryck SM, Treiber N, Meister G, Sumazin P, Zhang C. LIN28 selectively modulates a subclass of let-7 microRNAs. *Mol Cell* 2018;71:271–83 e275.
- [30] Uhlen M, Fagerberg L, Hallstrom BM, Lindskog C, Oksvold P, Mardinoglu A, Sivertsson A, Kampf C, Sjostedt E, Asplund A, et al. Proteomics. Tissue-based map of the human proteome. *Science* 2015;347:1260419.
- [31] Uhlen M, Bjorling E, Agaton C, Szigyarto CA, Amini B, Andersen E, Andersson AC, Angelidou P, Asplund A, Asplund C, et al. A human protein atlas for normal and cancer tissues based on antibody proteomics. *Mol Cell Proteomics* 2005;4:1920–32.
- [32] Sjostedt E, Zhong W, Fagerberg L, Karlsson M, Mitsios N, Adori C, Oksvold P, Edfors F, Limiszewska A, Hikmet F, et al. An atlas of the protein-coding genes in the human, pig, and mouse brain. *Science* 2020;367(6482) eaay5947. doi:10.1126/science.aya5947.
- [33] Loughlin FE, Gebert LF, Towbin H, Brunschweiger A, Hall J, Allain FH. Structural basis of pre-let-7 miRNA recognition by the zinc knuckles of pluripotency factor Lin28. *Nat Struct Mol Biol* 2011;19:84–9.
- [34] Hannus M, Beitzinger M, Engelmann JC, Weickert MT, Spang R, Hannus S, Meister G. siPools: highly complex but accurately defined siRNA pools eliminate off-target effects. *Nucleic Acids Res* 2014;42:8049–61.

- [35] Bahnassy AA, Zekri AR, Loutfy SA, Mohamed WS, Moneim AA, Salem SE, Sheta MM, Omar A, Al-Zawahry H. The role of cyclins and cyclin dependent kinases in development and progression of hepatitis C virus-genotype 4-associated hepatitis and hepatocellular carcinoma. *Exp Mol Pathol* 2011;91:643–52.
- [36] Masaki T, Shiratori Y, Rengifo W, Igarashi K, Yamagata M, Kurokochi K, Uchida N, Miyauchi Y, Yoshiji H, Watanabe S, et al. Cyclins and cyclin-dependent kinases: comparative study of hepatocellular carcinoma versus cirrhosis. *Hepatology* 2003;37:534–43.
- [37] Tang Z, Li C, Kang B, Gao G, Li C, Zhang Z. GEPPIA: a web server for cancer and normal gene expression profiling and interactive analyses. *Nucleic Acids Res* 2017;45:W98–W102.
- [38] Takahashi K, Koyama K, Ota Y, Iwamoto H, Yamakita K, Fujii S, Kitano Y. The interaction between long non-coding RNA HULC and microRNA-622 via transfer by extracellular vesicles regulates cell invasion and migration in human pancreatic cancer. *Front Oncol* 2020;10:1013.
- [39] Orlandella FM, Mariniello RM, Mirabelli P, De Stefano AE, Iervolino PLC, Lasorsa VA, Capasso M, Giannatiempo R, Rongo M, Incoronato M, et al. miR-622 is a novel potential biomarker of breast carcinoma and impairs motility of breast cancer cells through targeting NUAK1 kinase. *Br J Cancer* 2020;123:426–37.
- [40] Vigneron N, Vernon M, Meryet-Figuere M, Lambert B, Briand M, Louis MH, Krieger S, Joly F, Lheureux S, Blanc-Fournier C, et al. Predictive relevance of circulating miR-622 in patients with newly diagnosed and recurrent high-grade serous ovarian carcinoma. *Clin Chem* 2020;66:352–62.
- [41] Liu C, Min L, Kuang J, Zhu C, Qiu XY, Zhu L. Bioinformatic identification of miR-622 key target genes and experimental validation of the miR-622-RNF8 axis in breast cancer. *Front Oncol* 2019;9:1114.
- [42] Fang Y, Sun B, Wang J, Wang Y. miR-622 inhibits angiogenesis by suppressing the CXCR4-VEGFA axis in colorectal cancer. *Gene* 2019;699:37–42.
- [43] Dietrich P, Kuphal S, Spruss T, Hellerbrand C, Bosserhoff AK. MicroRNA-622 is a novel mediator of tumorigenicity in melanoma by targeting Kirsten rat sarcoma. *Pigment Cell Melanoma Res* 2018;31:614–29.
- [44] Song C, Lu P, Shi W, Sun G, Wang G, Huang X, Wang Z, Wang Z. MiR-622 functions as a tumor suppressor and directly targets E2F1 in human esophageal squamous cell carcinoma. *Biomed Pharmacother* 2016;83:843–9.
- [45] Huntzinger E, Izaurralde E. Gene silencing by microRNAs: contributions of translational repression and mRNA decay. *Nat Rev Genet* 2011;12:99–110.
- [46] Gerard C, Di-Luoffo M, Gonay L, Caruso S, Couchy G, Loriot A, Castven D, Tao J, Konobrocka K, Cordi S, et al. Dynamics and predicted drug response of a gene network linking dedifferentiation with beta-catenin dysfunction in hepatocellular carcinoma. *J Hepatol* 2019;71:323–32.
- [47] Tian N, Shangguan W, Zhou Z, Yao Y, Fan C, Cai L. Lin28b is involved in curcumin-reversed paclitaxel chemoresistance and associated with poor prognosis in hepatocellular carcinoma. *J Cancer* 2019;10:6074–87.
- [48] Cheng SW, Tsai HW, Lin YJ, Cheng PN, Chang YC, Yen CJ, Huang HP, Chuang YP, Chang TT, Lee CT, et al. Lin28B is an oncofetal circulating cancer stem cell-like marker associated with recurrence of hepatocellular carcinoma. *PLoS One* 2013;8:e80053.
- [49] Xu WP, Yi M, Li QQ, Zhou WP, Cong WM, Yang Y, Ning BF, Yin C, Huang ZW, Wang J, et al. Perturbation of microRNA-370/Lin-28 homolog A/nuclear factor kappa B regulatory circuit contributes to the development of hepatocellular carcinoma. *Hepatology* 2013;58:1977–91.
- [50] Guo Y, Chen Y, Ito H, Watanabe A, Ge X, Kodama T, Aburatani H. Identification and characterization of lin-28 homolog B (LIN28B) in human hepatocellular carcinoma. *Gene* 2006;384:51–61.
- [51] Hilmi M, Neuzillet C, Calderaro J, Lafdil F, Pawlotsky JM, Rousseau B. Angiogenesis and immune checkpoint inhibitors as therapies for hepatocellular carcinoma: current knowledge and future research directions. *J Immunother Cancer* 2019;7:333.
- [52] Roviello G, Sohbani N, Petrioli R, Rodriquenz MG. Ramucirumab as a second line therapy for advanced HCC: a significant achievement or a wasted opportunity for personalised therapy? *Invest New Drugs* 2019;37:1274–88.
- [53] Morse MA, Sun W, Kim R, He AR, Abada PB, Mynderse M, Finn RS. The role of angiogenesis in hepatocellular carcinoma. *Clin Cancer Res* 2019;25:912–20.
- [54] Petrillo M, Patella F, Pesapane F, Suter MB, Ierardi AM, Angileri SA, Floridi C, de Filippo M, Carrafiello G. Hypoxia and tumor angiogenesis in the era of hepatocellular carcinoma transarterial loco-regional treatments. *Future Oncol* 2018;14:2957–67.
- [55] Sonbol MB, Riaz IB, Naqvi SAA, Almqvist DR, Mina S, Almasri J, Shah S, Almader-Douglas D, Uson Junior PLS, Mahipal A, et al. Systemic therapy and sequencing options in advanced hepatocellular carcinoma: a systematic review and network meta-analysis. *JAMA Oncol* 2020;6:e204930.
- [56] Wang R, Ma Q, Ji L, Yao Y, Ma M, Wen Q. miR-622 suppresses tumor formation by directly targeting VEGFA in papillary thyroid carcinoma. *Oncotarget Ther* 2018;11:1501–9.
- [57] Cheng CW, Chen PM, Hsieh YH, Weng CC, Chang CW, Yao CC, Hu LY, Wu PE, Shen CY. Foxo3a-mediated overexpression of microRNA-622 suppresses tumor metastasis by repressing hypoxia-inducible factor-1alpha in ERK-responsive lung cancer. *Oncotarget* 2015;6:44222–38.
- [58] Guo XB, Jing CQ, Li LP, Zhang L, Shi YL, Wang JS, Liu JL, Li CS. Down-regulation of miR-622 in gastric cancer promotes cellular invasion and tumor metastasis by targeting ING1 gene. *World J Gastroenterol* 2011;17:1895–902.
- [59] Chen X, Du J, Zhu T. ING1a and ING1b different expressed in sporadic hepatocellular carcinoma. *Pathol Biol (Paris)* 2009;57:e17–21.
- [60] Zhang R, Luo H, Wang S, Chen Z, Hua L, Wang HW, Chen W, Yuan Y, Zhou X, Li D, et al. MiR-622 suppresses proliferation, invasion and migration by directly targeting activating transcription factor 2 in glioma cells. *J Neurooncol* 2015;121:63–72.
- [61] Rudalska R, Dauch D, Longerich T, McJunkin K, Wuestefeld T, Kang TW, Hohmeyer A, Pesci M, Leibold J, von Thun A, et al. In vivo RNAi screening identifies a mechanism of sorafenib resistance in liver cancer. *Nat Med* 2014;20:1138–46.
- [62] Berghoff AS, Bartsch R, Preusser M, Ricken G, Steger GG, Bago-Horvath Z, Rudas M, Streubel B, Dubsky P, Gnant M, et al. Co-overexpression of HER2/HER3 is a predictor of impaired survival in breast cancer patients. *Breast* 2014;23:637–43.
- [63] Murase H, Inokuchi M, Takagi Y, Kato K, Kojima K, Sugihara K. Prognostic significance of the co-overexpression of fibroblast growth factor receptors 1, 2 and 4 in gastric cancer. *Mol Clin Oncol* 2014;2:509–17.
- [64] Sultan AS, Brim H, Sheriff ZA. Co-overexpression of Janus kinase 2 and signal transducer and activator of transcription 5a promotes differentiation of mammary cancer cells through reversal of epithelial-mesenchymal transition. *Cancer Sci* 2008;99:272–9.
- [65] Wang L, Shi S, Guo Z, Zhang X, Han S, Yang A, Wen W, Zhu Q. Overexpression of YAP and TAZ is an independent predictor of prognosis in colorectal cancer and related to the proliferation and metastasis of colon cancer cells. *PLoS One* 2013;8:e65539.
- [66] Stumm G, Eberwein S, Rostock-Wolf S, Stein H, Pomer S, Schlegel J, Waldherr R. Concomitant overexpression of the EGFR and erbB-2 genes in renal cell carcinoma (RCC) is correlated with dedifferentiation and metastasis. *Int J Cancer* 1996;69:17–22.
- [67] Lin S, Gregory RI. Identification of small molecule inhibitors of Zcchc11 TUTase activity. *RNA Biol* 2015;12:792–800.
- [68] Bauer R, Valletta D, Bauer K, Thasler WE, Hartmann A, Muller M, Reichert TE, Hellerbrand C. Downregulation of P-cadherin expression in hepatocellular carcinoma induces tumorigenicity. *Int J Clin Exp Pathol* 2014;7:6125–32.
- [69] Lee SM, Schelcher C, Demmel M, Hauner M, Thasler WE. Isolation of human hepatocytes by a two-step collagenase perfusion procedure. *J Vis Exp* 2013.
- [70] Dietrich P, Gaza A, Wormser L, Fritz V, Hellerbrand C, Bosserhoff AK. Neuroblastoma RAS viral oncogene homolog (NRAS) is a novel prognostic marker and contributes to sorafenib resistance in hepatocellular carcinoma. *Neoplasia* 2019;21:257–68.
- [71] Thasler WE, Weiss TS, Schillhorn K, Stoll PT, Irrgang B, Jauch KW. Charitable state-controlled foundation human tissue and cell research: ethic and legal aspects in the supply of surgically removed human tissue for research in the academic and commercial sector in Germany. *Cell Tissue Bank* 2003;4:49–56.

- [72] Schiffner S, Brauner BM, de Jel MM, Coupland SE, Tamm ER, Bosserhoff AK. Tg(Grm1) transgenic mice: a murine model that mimics spontaneous uveal melanoma in humans? *Exp Eye Res* 2014;127:59–68.
- [73] Torres M, Becquet D, Guillen S, Boyer B, Moreno M, Blanchard MP, Franc JL, Francois-Bellan AM. RNA pull-down procedure to identify RNA targets of a long non-coding RNA. *J Vis Exp* 2018(134):57379. doi:10.3791/57379.
- [74] Dietrich P, Wormser L, Fritz V, Seitz T, De Maria M, Schambony A, Kremer AE, Gunther C, Itzel T, Thasler WE, et al. Molecular crosstalk between Y5 receptor and neuropeptide Y drives liver cancer. *J Clin Invest* 2020;130:2509–26.
- [75] Dietrich P, Hellerbrand C, Bosserhoff A. The Delta Subunit of Rod-Specific Photoreceptor cGMP Phosphodiesterase (PDE6D) Contributes to Hepatocellular Carcinoma Progression. *Cancers (Basel)* 2019;11(3):398. doi:10.3390/cancers11030398.
- [76] Voller D, Reinders J, Meister G, Bosserhoff AK. Strong reduction of AGO2 expression in melanoma and cellular consequences. *Br J Cancer* 2013;109:3116–24.
- [77] Bosserhoff AK, Ellmann L, Kuphal S. Melanoblasts in culture as an in vitro system to determine molecular changes in melanoma. *Exp Dermatol* 2011;20:435–40.
- [78] Schiffner S, Zimara N, Schmid R, Bosserhoff AK. p54nrb is a new regulator of progression of malignant melanoma. *Carcinogenesis* 2011;32:1176–82.
- [79] Franken NA, Rodermond HM, Stap J, Haveman J, van Bree C. Clonogenic assay of cells in vitro. *Nat Protoc* 2006;1:2315–19.
- [80] Mathews DH, Disney MD, Childs JL, Schroeder SJ, Zuker M, Turner DH. Incorporating chemical modification constraints into a dynamic programming algorithm for prediction of RNA secondary structure. *Proc Natl Acad Sci U S A* 2004;101:7287–92.